ARTICLES

A CASSCF and CASPT2 Study on the Excited States of *s-trans*-Formaldazine

Cheng Luo, Xue-mei Duan, Jing-yao Liu, and Ze-sheng Li*

Institute of Theoretical Chemistry, State Key Laboratory of Theoretical and Computational Chemistry, Jilin University, Changchun 130023, People's Republic of China

Received: December 11, 2007; Revised Manuscript Received: July 21, 2008

The low-lying excited states of *s-trans*-formaldazine ($H_2C{=}N{-}N{=}CH_2$) have been investigated using the complete active space self-consistent field (CASSCF) and the multiconfigurational second-order perturbation (CASPT2) methods. The vertical excitation energies have been calculated at the state-average CASSCF and multistate CASPT2 levels employing the cc-pVTZ basis set. The photodissociation mechanisms starting from the S_1 state have been determined. The lowest energy points along the seams of surface intersections have been located in both the Franck−Condon region and the N−N dissociation pathway in the S_1 state. Once the system populates the S_1 state, in the viewpoint of energy, the radiationless decay via $S_1/S_0(3)$ conical intersection followed by the N−N bond fission in the ground-state is more favorable in comparison with the N−N dissociation process in the S_1 state. A three-surface crossing region ($S_1/T_1/T_2$), where the S_1, T_1, and T_2 states intersect, was also found. However, the intersystem crossing process via $S_1/T_1/T_2$ is not energetically competitive with the internal conversion via $S_1/S_0(3)$.

Introduction

Formaldazine (2,3-diaza-1,3-butadiene, methanal azine, $H_2C{=}N{-}N{=}CH_2$), an analog of 1,3-butadiene, is the simplest member in the acyclic azine family. Since being first synthesized by Neureiter in 1959,[1] formaldazine has received particular interest as a stable dimer and a source[2] of methyleneiminyl (methylene amidogen, H_2CN) radical. The H_2CN radical is considered to be an intermediate in the combustion and decomposition of nitramine propellants,[3−8] and play an important role in the chemistry of extraterrestrial atmospheres.[4,9,10]

The equilibrium structures of formaldazine in the ground-state have been studied by both experimental[11−14]and theoretical[15,16] approaches. Early IR and microwave spectra indicated a cis structure of formaldazine with respect to the N−N bond.[11] However, on the basis of more extensive data of IR and Raman spectra, the trans structure was proposed to be more stable than the cis one.[12,13] In addition, the latter experiment[13] showed that there is a gauche conformer at room temperature. Through the electron diffraction investigations, Hagen et al.[14] suggested that the molecules exist as a mixture of trans and gauche conformers, and the trans structure is more stable than the gauche one. The energy barrier for the isomerization between the trans and gauche conformers was predicted to be 1.50 ± 0.74 kcal mol^{-1}.[14] The theoretical studies showed that there exist a series of gauche structures, the relative energies of which are in the range of 2.99−3.59 kcal mol^{-1} as compared with the trans structure.[15]

Ogilvie and Horne[16] studied the ultraviolet−visible absorption spectrum of formaldazine from 14 000 to 52 500 cm^{-1}. It was exhibited that there are three main absorption bands. The first absorption band centered at ∼34 500 cm^{-1} (4.28 eV) is completely diffuse and has no fine vibrational structure. The second band is around 44 150 cm^{-1}(5.47 eV). The third band, the most intense one, centers at ∼51 700 cm^{-1} (6.41 eV) with an apparent shoulder near 50 400 cm^{-1} (6.25 eV). The three bands were experimentally observed to have oscillator strengths of ∼0.0005, ∼0.003, and ≥0.16, respectively. They were assigned to the $\pi^* \leftarrow n$, $\sigma_{(CH)}^* \leftarrow \pi$, and $\pi^* \leftarrow \pi$ transitions by Ogilvie and Horne.[16]

The photodecomposition processes of azine compounds have been studied extensively in experiments.[2,16,18−22] Ogilvie and Horne[16] measured the transient absorption spectra of the decomposition products during the flash photolysis process of formaldazine using the double-beam prism spectrophotometer technique. No other signals were detected besides H_2CN from 210 to 650 nm, with an exception of a weak spectrum of CH_3 at 215 nm. After flash photolysis, the major products were collected and analyzed to be hydrogen cyanide, ammonia, ethane, methane, and ethyne in the order of decreasing abundance, and a trace of diazomethane was also found. Hydrogen or nitrogen was not observed in their experiments.[16] Horne and Norrish[2] studied the flash photolysis and the continuous photolysis of formaldazine at 253.7 nm. They proposed the following mechanisms:

$$FA + h\upsilon \rightarrow FA_\upsilon^* \quad (1)$$

$$FA_v^* \rightarrow CH_2N\cdot + CH_2N\cdot \quad (2)$$

$$FA_v^* \rightarrow CH_2NNCH\cdot + H \quad (3)$$

$$FA_v^* \rightarrow CCH_2N_2 + CH_2: \quad (4)$$

$$FA_v^* + M \rightarrow FA + M \quad (5)$$

$$CH_2N\cdot + CH_2N\cdot \rightarrow HCN + CH_2NH \quad (6)$$

* Corresponding author. Fax: +86-431-88498026; e-mail: zeshengli@mail.jlu.edu.cn.

10.1021/jp805081h CCC: $40.75
Published on Web 08/30/2008

$$CH_2N\cdot + CH_2N\cdot \rightarrow FA \quad (7)$$

$$6CH_2NH \rightarrow (CH_2)_6N_4 + 2NH_3 \quad (8)$$

where FA, FA_v*, and M denote formaldazine, vibronically excited formaldazine, and a third body, respectively. On the basis of the detection of methyleneiminyl signal, the marked effect, as well as the consumption of nitric oxide in the photolysis, the photodissociation process is predominated by a radical mechanism. No evidence proved the occurrence of reaction 3. The methane and diazomethane were also detected and attributed to reaction 4. Hydrogen cyanide, the major gaseous product, was considered to derive from the disproportionation reaction of methyleneiminyl radicals as represented in reaction 6. The approximate ratio between hydrogen cyanide and ammonia was 3.[2] The unimolecular decay processes for the photodissociation of matrix-isolated formaldazine were examined later employing electron spin resonance spectrum.[21] The methyleneiminyl radical was detected at wavelengths shorter than 320 nm.[21] Recently, Felder[22] investigated the 193 nm photodissociation process of formaldazine under collisionless conditions by measuring the molecular beam photofragment translational spectroscopy. Formaldazine was shown to dissociate primarily to two methyleneiminyl radicals on the time scale of $\leq 10^{-12}$ s. The methyleneiminyl radical undergoes a secondary dissociation step in which one of the CH bonds splits. Neither reaction 4 nor reaction 6 was found in Felder's experiment.[22]

To our knowledge, no theoretical investigation on the excited states has been reported to account for the photochemical processes of formaldazine. In the present paper, the characters of the potential energy surfaces of the low-lying excited states as well as the ground-state have been investigated. The mechanisms of the dissociation processes have been determined on the basis of the calculated potential energy surfaces and their intersections.

Computational Details

The stationary structures of formaldazine in the S_0, S_1, S_2, T_1, and T_2 states were optimized using the complete active space self-consistent field (CASSCF)[23] method with the cc-pVTZ basis set.[24] Once convergence was reached, the harmonic frequencies were analyzed to confirm the obtained geometry to be a minimum or a first-order saddle point, and the frequencies were not scaled. In order to consider the dynamic fractions of the correction energies for the stationary points, the single-point energies were refined by means of the multistate extension of multiconfigurational second-order perturbation approach (MS-CASPT2),[25] which takes the CASSCF wave functions as a reference in the second-order perturbation treatment. To minimize the effect of intruder states,[26] the level-shift technique was used when needed. To confirm the right connective relationships between transition states and minima (or dissociation products), the minimum energy pathway (MEP) calculations were performed at the CASSCF level. For the lowest triplet surface, the B3LYP[27,28] and MP2[29] calculations were also performed as a useful complement to the CASSCF method.

The selection of the active space is a crucial step for the CASSCF and CASPT2 calculations. For the ground state *s-trans*-formaldazine which has C_{2h} symmetry, the electronic configuration is given by $(1a_g)^2$, $(1b_u)^2$, $(2b_u)^2$, $(2a_g)^2$, $(3a_g)^2$, $(3b_u)^2$, $(4a_g)^2$, $(4b_u)^2$, $(5a_g)^2$, $(5b_u)^2$, $(6a_g)^2$, $(1a_u)^2$, $(6b_u)^2$, $(7a_g)^2$, $(1b_g)^2$, $(2a_u)^0$, $(7b_u)^0$, $(8a_g)^0$, $(2b_g)^0$, $(8b_u)^0$, $(9a_g)^0$, $(10a_g)^0$... In our calculations for the stationary points, the selected active space is comprised of $(5a_g)^2$, $(5b_u)^2$, $(6a_g)^2$, $(1a_u)^2$, $(6b_u)^2$, $(7a_g)^2$, $(1b_g)^2$, $(2a_u)^0$, $(7b_u)^0$, $(8a_g)^0$, $(2b_g)^0$, that is, 14 electrons in 11 orbitals, which will be referred to as CASSCF (14,11) hereafter. For convenience, the $1a_u$, $1b_g$, $2a_u$, and $2b_g$ orbitals, which are all provided with π orbital characters, will be referred to as π_1, π_2, π_3*, and π_4*, respectively.

The lowest energy points of the intersection seams between different electronic states including conical intersections (CIs) and intersystem crossing points (ISCs) have also been located. In order to get a balance between the precision and the computational cost, a reduced active space containing 10 electrons in eight orbitals was used for the location of the crossing points. This active space includes all the π type orbitals, the σ and σ* orbitals of the N−N bond, and the two lone pair orbitals of nitrogen atoms. At the ISCs, the spin−orbit coupling (SOC) constant between the singlet and triplet states has been calculated. The atomic mean field integrals (AMFI) method[30] and the effective one-electron Fock-type spin−orbit operator[31] are applied to simplify the treatment of the spin−orbit interaction.

The Gaussian 03 program[32] was used for the optimizations of the CIs as well as the B3LYP and MP2 calculations, while all the other calculations were carried out using the MOLCAS 6.2 program.[33]

Results and Discussion

Ground-State Equilibrium Geometry and Vertical Excitation Energies. From previous experimental[11,12,14] and theoretical[15,17] investigations, the most stable structure of formaldazine in the ground-state is the trans one with C_{2h} symmetry. The equilibrium geometry for *s-trans*-formaldazine obtained at the CASSCF(14,11)/cc-pVTZ level is presented in Figure 1 along with the atom labels and bond parameters. The calculated bond parameters are in good agreement with the corresponding experimental results in reference,[14] which means that our selection of the active space is reliable. A significant structural feature of *s-trans*-formaldazine is that the N−N distance of 1.398 Å is shorter than the typical N−N single bond length of 1.45 Å, while the C−N distance is 1.288 Å, slightly longer than the typical C−N double bond length of 1.25 Å. This structural characteristic can be attributed to the conjugation interaction between the two H_2CN moieties, which enhances the N−N bond and weakens the C−N bonds. The CNN, NCH (cis) and NCH (trans) angles are 111.5, 122.2, and 117.8°, respectively, which indicates that all the carbon and nitrogen atoms are sp^2 hybridized. It should be pointed out that the relatively large deviation of the CNN angle from the normal value of 120° is a result of the inequivalent hybridization of the nitrogen atom, that is, the repulsion between a lone-pair and a σ orbital is usually stronger than that between two σ orbitals.

In order to give an explicit theoretical interpretation of the gas phase UV spectrum, the vertical excitation energies (singlet and triplet) of formaldazine were calculated at the state average (SA)-CASSCF(14,11)/cc-pVTZ and MS-CASPT2(14,11)/cc-pVTZ levels. The relative energies of the involved states are listed in Table 1 along with the respective electric dipole transition oscillator strengths. Our calculations clearly show that the small frequency absorption band (34500 cm^{-1}) comes from the $1^1A_u \leftarrow 1^1A_g$ transition. The vertical excitation energies of this transition are predicted to be 4.01 and 3.62 eV at the CASSCF and CASPT2 levels, respectively, with the calculated oscillator strength being 0.00506. Through analyzing the coefficients of the CASSCF electronic configurations and the relevant molecular orbitals, it is concluded that the principal promotion of this transition is from the nitrogen lone-pair orbital to the π_3* orbital. The middle band (44150 cm^{-1}) corresponds to the $1^1B_g \leftarrow 1^1A_g$ transition. The CASSCF and CASPT2

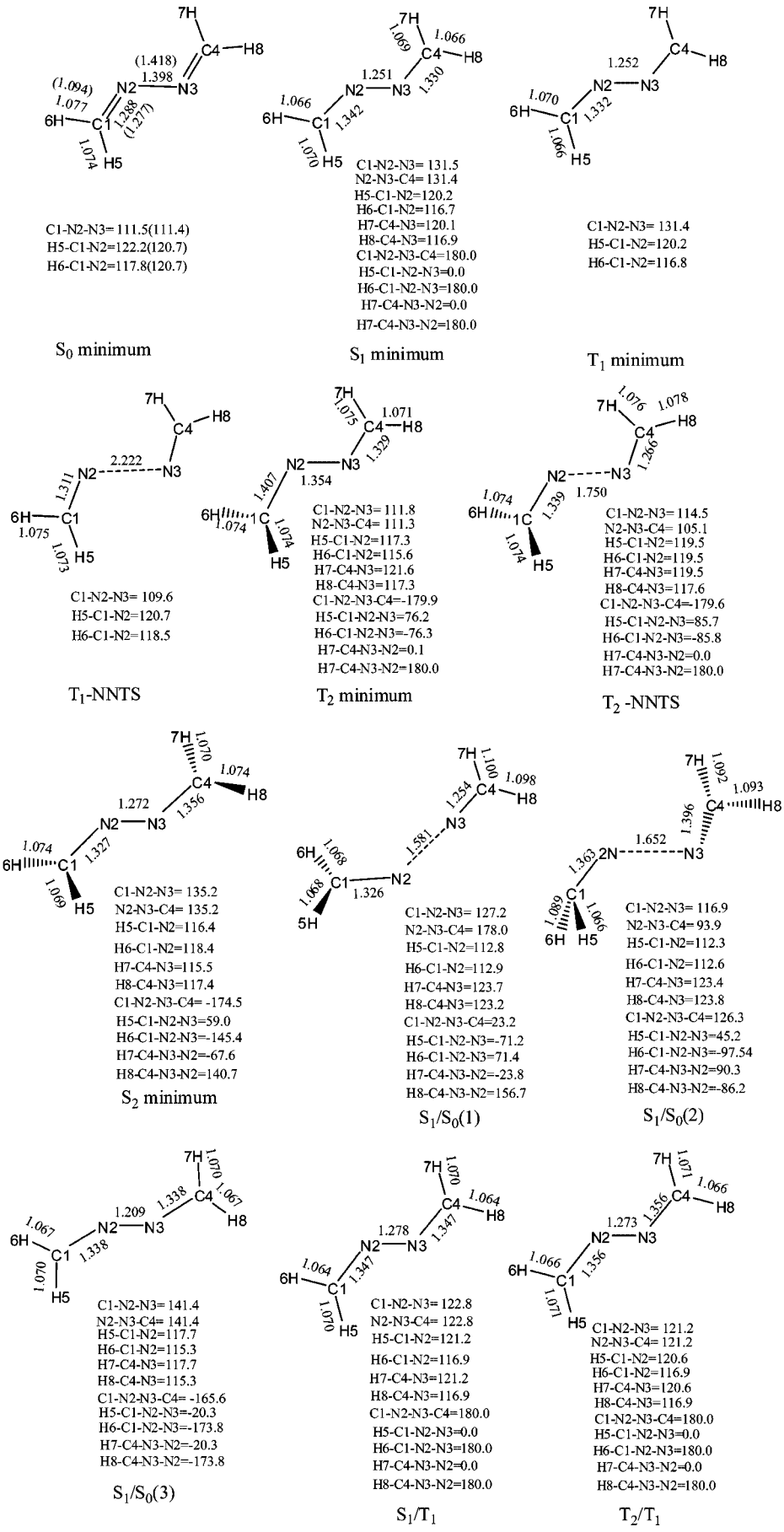

Figure 1. Schematic structures of stationary points in different electronic states with the CASSCF(14e,11o)/cc-pVTZ bond parameters and structures of surface crossing points with the CASSCF(10e,8o)/cc-pVTZ bond parameters. The values in parentheses are experimental values. (Bond lengths in angstroms and bond angles in degrees).

TABLE 1: SA-CASSCF and MS-CASPT2 Energies of the Vertical Transitions of Formaldazine

state	ΔE_{CASSCF}[a]	ΔE_{CASPT2}[b]	Rw[c]	f[d]	config[e]	weight[f]
1^1A_g (S_0)	0	0	0.86		2220 20 220 20	0.86
1^1A_u (S_1)	4.01	3.62	0.85	0.00506	22u0 2d 220 20	0.83
1^1B_g (S_2)	5.90	5.46	0.85	0.00000	2220 2u 2d0 20	0.17
					22u0 20 220 2d	0.64
1^1B_u (S_3)	8.54	6.40	0.82	0.76518	2220 2u 220 d0	0.89
1^3A_u (T_1)	3.69	3.39	0.85		22u0 2u 220 20	0.83
1^3B_u (T_2)	3.25	3.70	0.86		2220 2u 220 u0	0.83

[a] Relative SA-CASSCF(14e,11o)/cc-pVTZ energies in eV. [b] Relative MS-CASPT2(14e,11o)/cc-pVTZ energies in eV, with the level shift value equal to 0.2 hartree. [c] Reference weight of the configuration. [d] Oscillator strength in au. [e] CASSCF configurations of the weight larger than 0.1; the order of the irreducible representation is a_g, a_u, b_u, and b_g; u or d represents spin up or down. [f] Weight of the CASSCF configuration.

vertical excitation energies are 5.90 and 5.46 eV, respectively. The occupied numbers of the natural orbitals for the 1^1B_g state are shown as follows: $(5a_g)^{1.97}$, $(5b_u)^{1.99}$, $(6a_g)^{2.00}$, $(1a_u)^{1.95}$, $(6b_u)^{1.78}$, $(7a_g)^{1.21}$, $(1b_g)^{1.83}$, $(2a_u)^{0.44}$, $(7b_u)^{0.03}$, $(8a_g)^{0.01}$, $(2b_g)^{0.78}$. It is clear that the CASSCF wave function is provided with multireference character. Since the ground-state formaldazine presents C_{2h} geometry, this observed band corresponds to a symmetry-forbidden electronic transition. However, the experimentally observed oscillator strength of ~0.003 is derived from the effect of vibronic interaction, whose existence is usually proved by a distorted molecular structure in the corresponding excited state.[16] Our calculation shows that the C1N2N3C4, H5C1N2H6, and H7C4N3H8 dihedral angles in the 1^1B_g (S_2) equilibrium geometry are −174.5, 155.6, and −151.6°, respectively. The C_{2h} symmetry of the S_0 minimum is destroyed and becomes C_1 upon photoexcitation to S_2. According to our calculation, the strongest absorption peak is assigned to the $1^1B_u \leftarrow 1^1A_g$ transition with a large oscillator strength of 0.765. The vertical excitation energies calculated at the CASSCF and CASPT2 levels are 8.54 and 6.40 eV, respectively. This peak is assigned to the promotion of one electron from π_2 to π_3^*. By our calculations, the assignments of first and third bands are identical with those of Ogilvie and Horne's prediction,[16] while the second band is reassigned.

The N−N Bond Fissions in the S_0, S_1, T_1, and T_2 States. In the ground state, the N−N bond fission produces two H_2CN (1^2B_2) radicals. No transition state was found on the dissociation pathway. The dissociation energy is 2.28 eV at the CASPT2/cc-pVTZ level (see Table 2). For 1,3-butadiene ($CH_2CHCHCH_2$) and glyoxal (CHOCHO), two isoelectronic bodies of formaldazine that have similar 1,3-conjugation structures, the dissociations along their center C−C bonds also occur without transition states in the S_0 states.[34,35]

The optimized structure for S_1 minimum possesses C_s symmetry, with all the atoms in the molecular plane, which is consistent with the experimental prediction.[16] As shown in Figure 1, the N−N bond length is 1.251 Å, 0.147 Å shorter than the corresponding value in S_0 minimum, while the C1−N2 (C4−N3) bond length is 1.342 (1.330) Å, 0.054 (0.042) Å longer than that of S_0 minimum. The CNN angle of 131.4° (or 131.5°) in S_1 differs significantly from 111.5° in S_0. It is clear that the structural changes are caused by the $\pi_3^* \leftarrow n$ electronic transition, since the π_3^* orbital has antibonding nature over the two C−N bond regions and bonding nature over the N−N bond region, respectively. At the CASPT2 level, the S_1 minimum lies 2.32 eV above the S_0 minimum and 1.30 eV below the S_1 Franck−Condon (FC) point.

TABLE 2: CASSCF and CASPT2 Energies of Critical Points of Formaldazine

geometry	ΔE_{CASSCF}[a]	ΔE_{CASPT2}[b]	Rw[c]	ZPE[d]
S_0 (1^1A_g) minimum	0	0	0.85	0
S_1 (1^1A_u) minimum	3.02	2.32	0.84	−0.09
T_1 (1^3A_u) minimum	3.06	2.16	0.84	−0.15
T_1-NNTS	6.76	5.79	0.82	−0.17
T_2 (1^3B_u) minimum	2.57	2.64	0.85	−0.13
T_2-NNTS	3.26	3.12	0.84	−0.18
$H_2CN(1^2B_2)+H_2CN(1^2B_2)$	1.80	2.28	0.85	−0.28
$H_2CN(1^2B_2)+H_2CN(1^2B_1)$	6.34	5.81	0.84	−0.27
$S_1/S_0(1)$	6.51	6.14	0.84	
$S_1/S_0(2)$	6.42	5.99	0.83	
$S_1/S_0(3)$	3.58	2.45	0.83	
$S_1/T_1/T_2$	3.26	3.18	0.85	

[a] Relative CASSCF(14e,11o)/cc-pVTZ energies in eV. [b] Relative CASPT2(14e,11o)/cc-pVTZ energies in eV, with the level shift value equal to 0.0 hartree. [c] Reference weight of the configuration. [d] Zero point vibrational energies at the CASSCF(14e,11o)/cc-pVTZ level in eV.

On the N−N bond dissociation pathway in S_1, every effort to locate a transition state failed. The optimization always leads the system to a particular region where the single state wave function is hard to converge. It is found that the S_1 and S_0 surfaces approach each other in this region, which implies that surface crossings between S_1 and S_0 are likely to occur on the S_1 N−N dissociation pathway. The optimizations of the S_1/S_0 surface intersections were carried out at the SA-CASSCF(10,8)/cc-pVTZ level. Two S_1/S_0 CIs, referred to as $S_1/S_0(1)$ and $S_1/S_0(2)$, were obtained. As shown in Figure 1, the N−N distances in $S_1/S_0(1)$ and $S_1/S_0(2)$ are 1.581 and 1.652 Å, respectively. Considering the N−N distance, the internal conversion via $S_1/S_0(1)$ would occur prior to that via $S_1/S_0(2)$. Funneling through $S_1/S_0(1)$, two H_2CN (1^2B_2) radicals would be yielded. It is also possible for a vibrationally hot ground-state parent molecule to be produced through the nonradiative decay process.

In the triplet manifolds of formaldazine, the situation seems a little complicated. The two lowest lying triplet states are the 1^3A_u and 1^3B_u states, which originate from the $\pi_3^* \leftarrow n$ and $\pi_3^* \leftarrow \pi_2$ transitions, respectively, and will be referred to as $^3n\pi^*$ and $^3\pi\pi^*$ states hereafter. The vertical excitation energies of the $^3n\pi^*$ and $^3\pi\pi^*$ states are 3.25 and 3.69 eV at the CASSCF(14,11) level, but become 3.70 and 3.39 eV at the CASPT2(14,11) level, respectively, reversed in energetic order. The CASSCF(14,11) calculations shows that the $^3\pi\pi^*$ equilibrium structure (T_2 minimum) has a near-C_s symmetry with two H atoms out of the molecular symmetry plane. The $^3\pi\pi^*$ adiabatic excitation energy is predicted to be 2.64 eV at the CASPT2 level. On the $^3\pi\pi^*$ N−N dissociation pathway, a transition state, referred to as T_2-NNTS, is located at the CASSCF(14,11) level. The MEP calculations starting from this point show that T_2-NNTS connects T_2 minimum and two H_2CN (1^2B_2) radicals. At the CASPT2 level, T_2-NNTS lies 0.48 eV above T_2 minimum, which indicates that once the system populates the $^3\pi\pi^*$ state, it is not hard to undergo the N−N fission. The $^3n\pi^*$ equilibrium geometry was originally optimized from the FC point using C_1 symmetry. Serious divergence of single state wave function was encountered during the optimization process due to the approaching of the two lowest lying triplet states. Our SA-CASSCF(10,8) calculation (without symmetry constraint) confirms that a CI between the $^3n\pi^*$ and $^3\pi\pi^*$ states, referred to as T_2/T_1, exists in the FC region, via which internal conversion between the two states would take place. Employing C_{2h} symmetry, the $^3n\pi^*$ equilibrium geometry

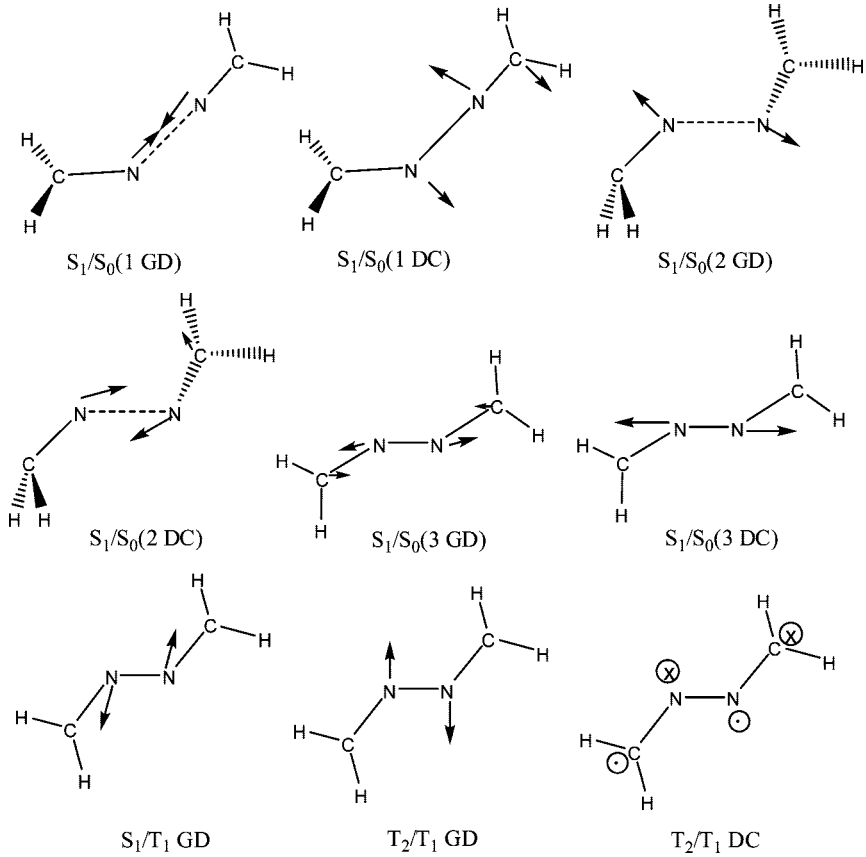

Figure 2. Schematic gradient difference (GD) and derivative coupling (DC) vectors at the surface crossing points ($S_1/S_0(1)$, $S_1/S_0(2)$, $S_1/S_0(3)$, S_1/T_1, and T_2/T_1).

(T_1 minimum) is obtained with no imaginary frequency. A transition state, referred to as T_1-NNTS, is located to connect the T_1 minimum on the reactant side and H_2CN (1^2B_2) + H_2CN (1^2B_1) on the product side. The CASSCF energy of T_1-NNTS is 6.76 eV with respect to the S_0 minimum, 0.42 eV above the adiabatic dissociation product. However, at the CASPT2 level, T_1-NNTS lies 5.79 eV above the S_0 minimum, 0.01 eV below the adiabatic dissociation product. Such a high barrier indicates that the N−N bond fission in $^3n\pi^*$ is hard to occur in comparison with that in $^3\pi\pi^*$. The B3LYP and the MP2 methods were also applied to investigate the $^3n\pi^*$ potential energy surface. At either the B3LYP/cc-pVTZ or the MP2/cc-pVTZ level, the equilibrium geometry was found to possess C_{2h} symmetry, and no transition state was found on the $^3n\pi^*$ N−N dissociation pathway.

Surfaces Intersections and Mechanistic Aspects. It is generally accepted that the reactions proceed mainly in the ground or lowest excited state, no matter which state is initially populated upon photoexcitation. Thus, our discussion on the reaction mechanisms will start from the S_1 state. The absorption band centered at 34 500 cm^{-1} is completely diffuse, indicating a progress of either a direct dissociation or a strong predissociation after photoexcitation to the S_1 state.[16] As mentioned above, on the S_1 N−N dissociation pathway lie $S_1/S_0(1)$ and $S_1/S_0(2)$ CIs, via which radiationless decays from S_1 to S_0 would occur efficiently. However, the relative energies of $S_1/S_0(1)$ and $S_1/S_0(2)$ are 6.14 and 5.99 eV at the CASPT2(14,11) level as compared with S_0 minimum, and both are inaccessible upon photoexcitation around 34 500 cm^{-1}. Accordingly, surface crossings in other regions where the S_1 state is intersected should be located in order to account for the predissociation processes.

The lowest energy points of the crossing seams between S_1 and S_0 (referred to as $S_1/S_0(3)$) and between S_1 and T_1 (referred to as S_1/T_1) in the FC region were optimized at the SA-CASSCF(10,8)/cc-pVTZ level with no symmetry constraint. The optimized $S_1/S_0(3)$ has a slightly distorted out-of-plane structure provided with C_2 symmetry. The bond lengths and bond angles of $S_1/S_0(3)$ are close to those of S_1 minimum except a shorter N−N distance of 1.209 Å and a larger CNN angle of 141.4°. The derivative coupling and the gradient difference vectors that form the branching space are plotted in Figure 2. The derivative coupling vector at $S_1/S_0(3)$ is mainly associated with the stretching motion of the N−N bond, leading to the S_1 minimum. The gradient difference vector corresponds mainly to the N−N elongation and the C−N shortening as well as the CNN bending motion, with the molecule moving along this vector resulting in the S_0 minimum. For the ISC, it is interesting that S_1/T_1 and T_2/T_1 are not distinguishable both structurally and energetically. The largest deviations of bond lengths and bond angles between S_1/T_1 and T_2/T_1 are less than 0.01 Å and 1.6°, respectively, and the CASPT2(14,11) energy difference in T_1 between the two geometries is smaller than 0.06 eV. Thus, this region can be considered as a region where three potential surfaces (S_1, T_1, and T_2) intersect. This is not surprising because the T_1 and T_2 surfaces are close to each other in the FC region. Actually, for a number of molecules that involve the $n\pi^*$ and $\pi\pi^*$ transitions upon photoexcitation, three-surface intersections have also been found near the FC region among the S_1, T_1, and T_2 states.[36−38]

Once the S_1 state, a bound excited state, is populated, it is hard to undergo the N−N fission process, as discussed above. However, the S_1 state may nevertheless be short-lived since it is intersected by other states where fragmentations can happen at lower energies. At the CASPT2(14,11) level, $S_1/S_0(3)$ lies 2.45 eV above the S_0 minimum, only 0.13 eV above the S_1 minimum. In the viewpoint of energy, the internal conversion

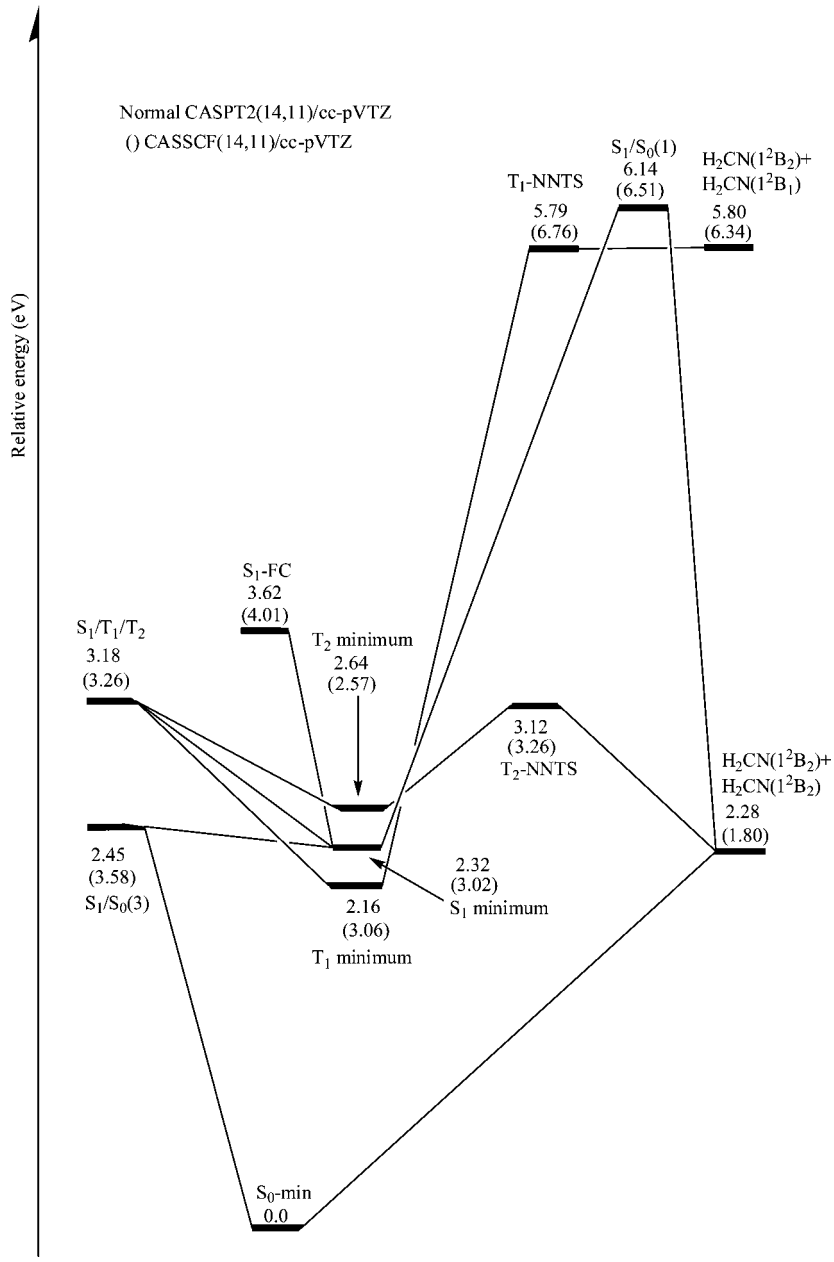

Figure 3. Schematic map of low-lying singlet and triplet surfaces of formaldazine. FC denotes the Franck−Condon point. S_x/S_y represents the CI between the S_x and S_y states. S_x/T_y represents the intersection point where intersystem crossing occurs between the S_x and T_y states.

via $S_1/S_0(3)$ is the most probable relaxation channel in S_1. As shown in Figure 3, the striking structural changes among S_0 minimum, S_1 minimum, and $S_1/S_0(3)$ are associated with the N−N bond and the CNN angle. Thus, it is reasonable to anticipate that the radiationless decay from S_1 to S_0 via $S_1/S_0(3)$ would produce a vibrationally hot ground-state molecule, with excitations mostly in the N−N stretching and the CNN bending modes. After decay to the ground state, the N−N bond is likely to cleave under the condition that abundant vibrational energy is accumulated over the N−N bond region, and two H_2CN (1^2B_2) radicals would be yielded. In comparison with the internal conversion via $S_1/S_0(3)$, the intersystem crossing via $S_1/T_1/T_2$ intersection is not likely to make significant contribution to the photodissociation dynamics of formaldazine because of the relatively high energy (3.18 eV above the S_0 minimum at the CASPT2 level), although the calculated norm of the SOC element is 19.5 cm^{-1} between S_1 and T_1. In fact, experiment on the flash photolysis of formaldazine at 253.7 nm^2 has shown that the carrier of the transient UV spectrum, i.e., methylene-iminyl radical, is not a metastable electronically excited species. The reaction channel involving the internal conversion from S_1 to S_0 and the subsequent dissociation in S_0 is consistent with the experimental finding.

Conclusion

The electronic absorption spectrum of *s-trans*-H_2CNNCH_2 has been investigated by means of the CASSCF and CASPT2 approaches. The three main absorption bands between 14 000 and 52 500 cm^{-1} have been reassigned to $n\pi^*$, a multireference, and $\pi\pi^*$ transitions, respectively. Three CIs have been located between the S_1 and S_0 states. One of them ($S_1/S_0(3)$) lies in the FC region, and has a fairly low energy (0.13 eV) with respect to the S_1 minimum. The internal conversion from S_1 to S_0 via $S_1/S_0(3)$ followed by the N−N dissociation in S_0 would be responsible for the vibrational diffuse nature in the UV spectrum.

A three-surface intersection ($S_1/T_1/T_2$) has been found; however, the relative energy of this point is too high for the intersystem crossing to compete with the internal conversion via $S_1/S_0(3)$. The N−N dissociation channel with the most possibility can be summarized as follows: $S_0 + h\nu \rightarrow S_1-FC \rightarrow S_1$ minimum $\rightarrow S_1/S_0(3) \rightarrow S_0$ minimum $\rightarrow 2H_2CN$ (1^2B_2).

Our theoretical results are consistent with the corresponding experiments and may be useful for further experimental studies about formaldazine and relevant azine molecules.

Acknowledgment. This work was supported by the National Science Foundation of China (20333050, 20673044), PCSIRT(IRT0625), Key subject of Science and Technology by Jilin Province.

References and Notes

(1) Neureiter, N. P. *J. Am. Chem. Soc.* **1959**, *81*, 2910.
(2) Horne, D. G.; Norrish, R. G. W. *Proc. R. Soc. London, Ser. A* **1970**, *315*, 301.
(3) Morgan, C. U.; Beyer, R. A. *Combust. Flame* **1979**, *36*, 99.
(4) Marston, G.; Stief, L. J. *Res. Chem. Intermed.* **1989**, *12*, 161.
(5) Alexander, M. H.; Dagdigian, P. J.; Jacox, M. E.; Kolb, C. E.; Melius, C. F.; Rabitz, H.; Smooke, M. D.; Tsang, W. *Prog. Energy Combust. Sci.* **1991**, *17*, 263.
(6) Adams, G. F.; Shaw, R. W. *Annu. Rev. Phys. Chem.* **1992**, *43*, 311.
(7) Rice, B. M.; Adams, G. F.; Page, M.; Thompson, D. L. J. *Phys. Chem.* **1995**, *99*, 5016.
(8) Teslja, A.; Dagdigian, P. J.; Banck, M.; Eisfeld, W. *J. Phys. Chem. A* **2006**, *110*, 7826.
(9) Marston, G.; Nesbitt, F. L.; Stief, L. J. *J. Chem. Phys.* **1989**, *91*, 3483.
(10) Nesbitt, F. L.; Marston, G.; Stief, L. J.; Wickramaaratchi, M. A.; Tao, W.; Klemm, R. B. *J. Phys. Chem.* **1991**, *95*, 7613.
(11) Ogelvie, J. F. *Chem. Commun.* **1965**, 359.
(12) Ogelvie, J. F.; Cole, K. C. *Spectrochim. Acta, Part A* **1971**, *27*, 877.
(13) Bodebey, V.; Nibler, J. W. *Spectrochim. Acta, Part A* **1973**, *29*, 645.
(14) Hagen, K.; Bondybey, V.; Hedberg, K. *J. Am. Chem. Soc.* **1977**, *95*, 1365.
(15) Bock, C. W.; George, P.; Trachtman, M. *J. Comput. Chem.* **1984**, *5*, 395.
(16) Ogilvie, J. F.; Horne, D. G. *J. Chem. Phys.* **1968**, *48*, 2248.
(17) Schmitz, B. K.; Euler, W. B. *J. Comput. Chem.* **1994**, *15*, 1163.
(18) Rice, F. O.; Glasebrook, A. L. *J. Am. Chem. Soc.* **1934**, *56*, 741.
(19) HorneD. G. Ph.D. Thesis, Cambridge University, 1966.
(20) Briton, R. K. *J. Am. Chem. Soc.* **1955**, *77*, 842.
(21) Kamachi, M.; Kuwata, K.; Murahashi, S. *J. Phys. Chem.* **1971**, *75*, 164.
(22) Felder, P.; Harrison, J. A.; Huber, J. R. *J. Phys. Chem.* **1991**, *95*, 1945.
(23) Roos, B. O. In *Advances in Chemical Physics; Ab Initio Methods in Quantum Chemistry II*; Lawley, K. P., Ed.; Wiley Chichester, England, 1987; Chapter 69, p399.
(24) Dunning, T. H. *J. Chem. Phys.* **1989**, *90*, 1007.
(25) Finley, J.; Malmqvist, P. Å.; Roos, B. O.; Serrano-Andrés, L. *Chem. Phys. Lett.* **1998**, *288*, 299.
(26) Such states, which were not included in the CASSCF configuration interaction but have energies within the range of the lowest CAS states, cause frequent problems in excited state calculations, since they often give small denominators and even, at particular geometries, singularities. We call these states intruders, by analogy to a similar phenomenon in multistate perturbation theory.
(27) Becke, A. D. *J. Chem. Phys.* **1993**, *98*, 1372.
(28) Lee, C.; Yang, W.; Parr, R. G. *Phys. Rev. B* **1998**, *37*, 785.
(29) Hehre, W. J.; Radom, L.; Schleyr, V. R.; Pople, J. A. *Ab Initio Molecular Orbital Theory*; Wiley: New York, 1986.
(30) Christiansen, O.; Gauss, J.; Schimmelpfennig, B. *Phys. Chem. Chem. Phys.* **2000**, *2*, 965.
(31) Hess, B. A.; Marian, C.; Wahlgren, U.; Gropen, O. *Chem. Phys. Lett.* **1996**, *251*, 365.
(32) (a) Frisch, M. J.; Trucks, G. W.; Schlegel, H. B.; Scuseria, G. E.; Robb, M. A.; Cheeseman, J. R.; Montgomery, J. A., Jr.; Vreven, T.; Kudin, K. N.; Burant, J. C.; Millam, J. M.; Iyengar, S. S.; Tomasi, J.; Barone, V.; Mennucci, B.; Cossi, M.; Scalmani, G.; Rega, N.; Petersson, G. A.; Nakatsuji, H.; Hada, M.; Ehara, M.; Toyota, K.; Fukuda, R.; Hasegawa, J.; Ishida, M.; Nakajima, T.; Honda, Y.; Kitao, O.; Nakai, H.; Klene, M.; Li, X.; Knox, J. E.; Hratchian, H. P.; Cross, J. B.; Bakken, V.; Adamo, C.; Jaramillo, J.; Gomperts, R.; Stratmann, R. E.; Yazyev, O.; Austin, A. J.; Cammi, R.; Pomelli, C.; Ochterski, J. W.; Ayala, P. Y.; Morokuma, K.; Voth, G. A.; Salvador, P.; Dannenberg, J. J.; Zakrzewski, V. G.; Dapprich, S.; Daniels, A. D.; Strain, M. C.; Farkas, O.; Malick, D. K.; Rabuck, A. D.; Raghavachari, K.; Foresman, J. B.; Ortiz, J. V.; Cui, Q.; Baboul, A. G.; Clifford, S.; Cioslowski, J.; Stefanov, B. B.; Liu, G.; Liashenko, A.; Piskorz, P.; Komaromi, I.; Martin, R. L.; Fox, D. J.; Keith, T.; Al-Laham, M. A.; Peng, C. Y.; Nanayakkara, A.; Challacombe, M.; Gill, P. M. W.; Johnson, B.; Chen, W.; Wong, M. W.; Gonzalez, C.; Pople, J. A. *Gaussian 03*, revision C.01; Gaussian, Inc.: Pittsburgh, PA, 2003. (b) Bearpark, M. J.; Robb, M. A.; Schlegel, H. B. *Chem. Phys. Lett.* **1994**, 223–269. (c) Yarkony, D. R. *J. Chem. Phys.* **1990**, *92*, 2457.
(33) Karlström, G.; Lindh, R.; Malmqvist, P. Å. *Comput. Mater. Sci.* **2003**, *28*, 222.
(34) Lee, H. Y.; Kislov, V. V.; Lin, S. H.; Mebel, A. M.; Neumark, D. M. *Chem.—Eur. J.* **2003**, *9*, 726.
(35) Li, Q. S.; Zhang, F.; Fang, W. H.; Yu, J. G. *J. Chem. Phys.* **2006**, *124*, 054324.
(36) Fang, W. H.; Phillips, D. L. *ChemPhysChem* **2002**, *3*, 889.
(37) Chen, X. B.; Fang, W. H. *J. Am. Chem. Soc.* **2004**, *126*, 8976.
(38) Cui, Q.; Morokuma, K. *J. Chem. Phys.* **1997**, *107*, 4951.

JP805081H